Theoretical and Computational Acoustics
D. Lee, Y-H Pao, M.H. Schultz, and Y-C Teng (Editors)

Acoustic Transient Signal Transfer Between Two Fluid-Filled Boreholes Embedded in a Horizontally Stratified Anisotropic Elastic Formation

Bastiaan P. de Hon
Laboratory of Electromagnetic Research
Department of Electrical Engineering
Centre for Technical Geoscience
Delft University of Technology
P.O. Box 5031, 2600 GA Delft, The Netherlands

Abstract: A method is presented to construct the transient acoustic pressure in a borehole due to the action of a volume injection source in another borehole in a typical cross-well seismic setting with a horizontally stratified anisotropic solid formation. The elastic wave motion in the formation is considered to be generated by distributed surface sources. Via an appropriate combination of a Laplace transformation with respect to time and Fourier transformations with respect to the horizontal coordinates, a matrix differential equation for the spectral acoustic state quantities is obtained. A so-called splitting matrix is introduced to decompose the spectral down- and up-going wavefield constituents. The generalized-ray constituents, representing the wave constituents that have undergone successive reflections and transmissions at the interfaces, are transformed back to the space-time domain with the aid of the modified Cagniard method. At the relatively low frequencies involved, the acoustic wave motion inside a fluid-filled borehole, is dominated by tube waves. The excitation and propagation properties of the tube wave are modeled by regarding the borehole as an acoustic waveguide with a compliant inner wall. The corresponding elastic wavefield quantities at the borehole wall serve as distributed surface sources that generate the elastic wave motion in the formation. The acoustic pressure on the axis of the receiving borehole is evaluated through a suitable application of the fluid/solid acoustic reciprocity theorem. Several of the physical phenomena described by the resulting expressions, are illustrated via numerical simulations.

1. INTRODUCTION

Acoustic signals, as measured in cross-hole seismic experiments involving volume injection sources and acoustic pressure receivers, contain strong tube-wave related phenomena. This was first recognized by White and Sengbush [1]. Of late, Dong and Toksöz [2] have analyzed a real cross-well data set, showing that most of the strong events in the data can only be explained if both the transmitting and the receiving holes are incorporated in the model. In particular, converted waves can be stronger than the primaries. Further, on account of recent measurements, the current opinion is that anisotropy should be included in the model.

To model the acoustic wave motion inside a fluid-filled borehole, the acoustic radiation emanating from such a borehole and the full cross-hole transfer of acoustic signals, a wide variety of modeling methods has been employed. Here, we mention the far-field asymptotic methods to determine the wavefield radiated into the formation — Lee and Balch [3] and Meredith [4]; the equivalent seismic source methods to determine the wavefield radiated into the formation — Kurkjian *et al.* [5]; the finite difference methods — Track and Daube[6]; and the hybrid space-time-domain methods, in which the final expression is assembled out of the solutions to subproblems

obtained by different techniques — White and Sengbush [1], Burridge *et al.* [7] De Hoop *et al.* [8] and Dong and Toksöz [2]. We refer to the De Hoop *et al.* [8] for a more detailed description of the literature.

In this paper, we present a method by which the transfer of transient tube-wave signals in cross-hole experiments can completely be calculated within a specified time window of observation. The major part of the analysis is performed in the spectral domain via an appropriate combination of a Laplace transformation with respect to time and Fourier transformations with respect to the horizontal spatial coordinates. The spectral domain solution is constructed in terms of generalized rays.

The analysis involves the following consecutive steps. First, we consider the spectral-domain down- and upward propagating wavefield quantities within a homogeneous anisotropic layer in the formation and their excitation by distributed borehole surface sources. We use the scattering matrix formalism to describe the interaction of the down- and up-going waves at the interfaces between two consecutive layers. Next, we employ a small parameter analysis to describe the low-frequency tube-wave motion in the borehole fluid, hereby addressing its dependence on the radial stiffness of the compliant inner borehole wall, its excitation by a point source of volume injection, and the influence of the presence of a concentric shell structure surrounding the borehole fluid on the radial stiffness of the inner wall and on the resulting wavefield quantities at the outer wall that determine the spectral-domain surface sources. Subsequently, we discuss how to apply a fluid/solid reciprocity theorem to express the spectral-domain received acoustic pressure in terms of the surface sources of the elastic wavefield incident on the receiving borehole and the surface sources of the applied auxiliary state. Next, we describe an alternative implementation of the modified Cagniard method, by which the transformation from the spectral domain to the space-time domain is carried out, yielding the desired transient cross-hole acoustic pressure Green's functions. Finally, the results of numerical simulations are used to illustrate the physical phenomena described by the method. We conclude with a discussion about the ramifications of the presented theory and results.

2. DESCRIPTION OF THE CONFIGURATION

We investigate theoretically the transient cross-hole signal transfer in a configuration consisting of two vertical, circularly cylindrical, fluid-filled boreholes embedded in a perfectly elastic, horizontally stratified, anisotropic solid formation. To specify the position in the configuration, we employ the coordinates $\{x_1, x_2, x_3\}$ with respect to a fixed, orthogonal, Cartesian frame of reference, with the origin $\mathcal{O}$ and the three mutually perpendicular base vectors $\{\mathbf{i}_1, \mathbf{i}_2, \mathbf{i}_3\}$ of unit length each. In the indicated order, the base vectors form a right-handed system. In accordance with the geophysical convention, $\mathbf{i}_3$ points vertically downwards. The subscript notation for Cartesian vectors and tensors is used. Lowercase Latin subscripts are used for this purpose; they are to be assigned the values 1, 2 and 3. Lowercase Greek subscripts are used to indicate the horizontal components of the Cartesian vectors and tensors; they are to be assigned the values 1 and 2. For the vertical component the subscript 3 is then written explicitly. To all repeated subscripts, the summation convention applies. Whenever appropriate, the position is also specified by the position vector $\mathbf{x} = x_p\mathbf{i}_p$. The time coordinate is denoted by t. Partial differentiation with respect to x_p is denoted by ∂_p, whereas ∂_t is a reserved symbol denoting partial differentiation with respect to time. In addition to using Cartesian vectors and tensors, we employ a matrix notation, in which we denote 6 by 6 matrices by capital sans serif characters, 3 by 3 submatrices of such matrices by plain capital characters, 6-vectors by lowercase boldface sans serif characters and 3-vectors by plain lowercase boldface characters, respectively. To evaluate the elastoacoustic radiation emanating from the source hole, we initially neglect the presence of the receiving hole. The support of the anisotropic solid formation is a connected open set of points represented by

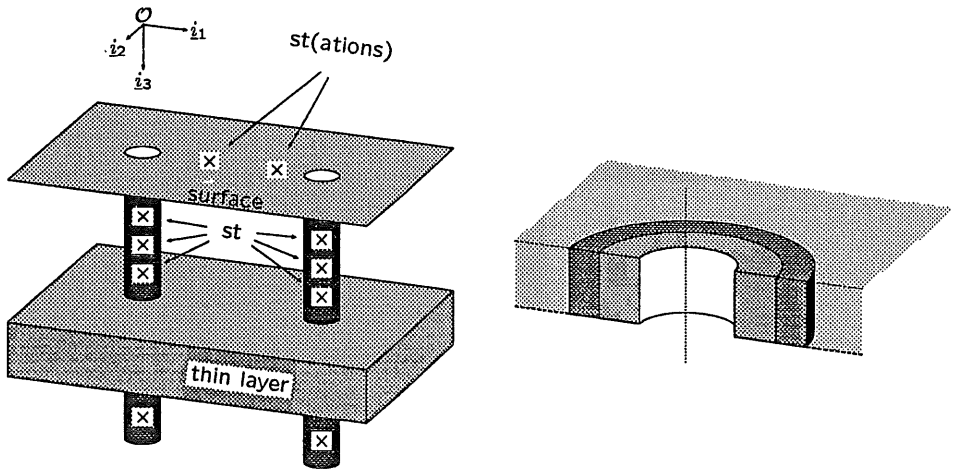

Figure 1: The illustration on the left shows a possible configuration; the illustration on the right shows the shell structure of a fluid-filled borehole.

the symbol $\mathcal{D}$. The closure of $\mathcal{D}$ constitutes the boundary of the formation, i.e., the outer wall of the vertical, circularly cylindrical, borehole and is denoted as $\partial\mathcal{B}^+$. The symbol $\boldsymbol{\nu}$ is used to denote the unit vector oriented along the inward normal to the boundary, i.e., into the formation. The solid configuration consists of a stack of plane layers with different anisotropic elastic material properties. These layers are assumed to be in rigid contact. The interfaces between the formation layers are located on the vertical levels $x_3 = x_{3;J}$ with $J = 0, 1, \ldots, M$ and $x_{3;M} = \infty$. The configuration may be bounded from above by a free surface, in which case $x_{3;0}$ is used to indicate the corresponding vertical level. Otherwise, we take $x_{3;0} = -\infty$. Further, the interval $\mathcal{I}_J = (x_{3;J-1}, x_{3;J})$ with $J = 1, 2, \ldots$ denotes an open subset of the x_3-axis, while the open subdomain $\mathcal{D}_J$ of $\mathcal{D}$ is defined as $\mathcal{D}_J = \{\mathbf{x}|\mathbf{x} \in \mathcal{D} \text{ and } x_3 \in \mathcal{I}_J\}$ The horizontal surface $\mathcal{S} = \mathcal{S}(x_3)$, represents the cross-section of the domain $\mathcal{D}$ and the horizontal plane at the vertical level x_3 with $x_3 \neq x_{3;J}$. Accordingly, the closure $\partial\mathcal{S}$ of $\mathcal{S}$ is the circle of intersection of the pertaining horizontal plane and the boundary $\partial\mathcal{B}^+$ of $\mathcal{D}$. At the instant $t = 0$ a point source of volume injection, located at $\mathbf{x} = \mathbf{x}^S$ on the axis of the source borehole, starts to generate the acoustic wave motion, which is initially at rest. An acoustic pressure point receiver located at $\mathbf{x} = \mathbf{x}^R$ on the axis of the receiving borehole measures the transferred acoustic signal. The domain occupied by the fluid column inside a borehole is denoted as $\mathcal{B}^-$, while b^- and Ω^- denote the pertaining radius and cross-sectional area, respectively. In between the fluid columns and the solid formation a finite system of concentric circularly cylindrical shells, representing casing, cementing, etc, may be present. The domain occupied by a borehole, including these shells, is denoted as $\mathcal{B}^+$, while b^+ and Ω^+ denote the pertaining radius and cross-sectional area, respectively. The different layers in the shell structure are assumed to be in rigid contact with one another and with the solid formation. The fluid/solid interface in a borehole is denoted as $\partial\mathcal{B}^-$. Whenever we have to distinguish between the source and receiving holes, we add the superscripts S and R to pertaining quantities. We have depicted a possible configuration in Figure 1.

3. THE ELASTIC WAVE MOTION IN A STRATIFIED ANISOTROPIC FORMATION

Below, we investigate the elastic wave motion in a general anisotropic, homogeneous and lossless subdomain $\mathcal{D}_J$, constituting a horizontal layer from which vertical circular cylindrical source hole is excluded, while the receiving hole is considered to be absent. We assume that the medium that occupies this subdomain of the configuration is initially at rest. In the absence of volume sources, the equation of motion and the deformation rate equation describing the elastic wave motion in a homogeneous solid domain are given by (cf. Van der Hijden [9])

$$-\Delta_{kmpq}\partial_m\tau_{pq} + \rho_{kp}\partial_t v_p = 0, \tag{1a}$$

$$\Delta_{ijpq}\partial_q v_p - \varsigma_{ijpq}\partial_t\tau_{pq} = 0, \tag{1b}$$

where τ_{pq} is the dynamic stress (Pa), v_k is the particle velocity (m/s), ρ_{kp} is the volume density of mass (kg/m^3) and ς_{ijpq} is the compliance (Pa^{-1}), respectively. Further, $\Delta_{ijpq} = \frac{1}{2}(\delta_{ip}\delta_{jq} + \delta_{iq}\delta_{jp})$ is the completely symmetric unit tensor of the rank 4 and δ_{ip} is the Kronecker unit tensor of the rank 2. The compliance is the inverse of the stiffness c_{kmij} (Pa), i.e., $c_{kmij}\varsigma_{ijpq} = \Delta_{kmpq}$. We require both the volume density of kinetic energy and the volume density of strain energy to be positive for a non-vanishing acoustic field. Hence, we demand that the inequalities $\rho_{kp}a_k a_p > 0$, $c_{kmij}b_{km}b_{ij} > 0$ and $\varsigma_{ijpq}b_{ij}b_{pq} > 0$ hold for all real non-vanishing vectors a_k and symmetric tensors b_{km}, respectively. Further, we confine ourselves to reciprocal media entailing that $\rho_{kp} = \rho_{pk}$, $c_{kmij} = c_{mkij} = c_{ijmk}$ and $\varsigma_{ijpq} = \varsigma_{jipq} = \varsigma_{pqji}$, respectively.

Our method of analysis involves the use of a unilateral Laplace transformation with respect to time and a Fourier transformation of the Radon type with respect to the spatial coordinates over a horizontal surface $\mathcal{S}$ with a circular boundary $\partial\mathcal{S}$. For any wavefield quantity Ψ and for any such horizontal surface, we have

$$\hat{\Psi}(x_k, s) = \int_{t=0^-}^{\infty} \exp(-st)\Psi(x_k, t)\,\mathrm{d}t \quad \text{and} \quad \tilde{\Psi}(\alpha_\mu, x_3, s) = \int_{x_\mu\in\mathcal{S}} \exp(is\alpha_\lambda x_\lambda)\hat{\Psi}(x_m, s)\,\mathrm{d}\Sigma, \tag{2}$$

in which s is taken real and positive so as to ensure causality, while $\alpha_\mu \in \mathbb{R}^2$. Then, for vanishing initial conditions, we have $\partial_t \to s$ and

$$\int_{x_\mu\in\mathcal{S}} \exp(is\alpha_\lambda x_\lambda)\partial_m\hat{\Psi}\,\mathrm{d}\Sigma = -is\alpha_\mu\delta_{m\mu}\tilde{\Psi} + \delta_{m3}\partial_3\tilde{\Psi} - \int_{x_\mu\in\partial\mathcal{S}} \hat{\Psi}\exp(is\alpha_\lambda x_\lambda)\nu_\mu\delta_{m\mu}\,\mathrm{d}\ell, \tag{3}$$

in which $\nu = \nu_\lambda \mathbf{i}_\lambda$ denotes the (in-plane) unit vector oriented along the *inward* normal to $\partial\mathcal{S}$ and we have used Gauss' theorem. As $\mathcal{S}$ is considered to be an open set, we inversely have

$$\hat{\Psi}(x_k, s) = \left(\frac{s}{2\pi}\right)^2 \int_{\alpha_\mu\in\mathbb{R}^2} \exp(-is\alpha_\lambda x_\lambda)\tilde{\Psi}(\alpha_\mu, x_3, s)\,\mathrm{d}\Sigma. \tag{4}$$

Upon applying the Laplace and Fourier transformations to Eq. (1), we arrive at

$$-\partial_3\Delta_{k3pq}\tilde{\tau}_{pq} + s\Delta_{k\mu pq}i\alpha_\mu\tilde{\tau}_{pq} + s\rho_{kp}\tilde{v}_p = \tilde{f}_k^{\partial\mathcal{B}^+}, \tag{5a}$$

$$\Delta_{ijp3}\partial_3\tilde{v}_p - s\Delta_{ijp\mu}i\alpha_\mu\tilde{v}_p - s\varsigma_{ijpq}\tilde{\tau}_{pq} = \Delta_{ijpq}\tilde{h}_{pq}^{\partial\mathcal{B}^+}. \tag{5b}$$

in which

$$\tilde{f}_k^{\partial\mathcal{B}^+} = -\int_{x_\mu\in\partial\mathcal{S}} \exp(is\alpha_\lambda x_\lambda)\Delta_{k\mu pq}\hat{\tau}_{pq}\nu_\mu\,\mathrm{d}\ell, \quad \text{and} \quad \tilde{h}_{ij}^{\partial\mathcal{B}^+} = \int_{x_\mu\in\partial\mathcal{S}} \exp(is\alpha_\lambda x_\lambda)\Delta_{ijpq}\hat{v}_p\nu_\mu\delta_{q\mu}\,\mathrm{d}\ell \tag{6}$$

are the spectral-domain boundary-surface-force source and boundary-surface source of deformation rate, respectively. As the state quantities in Eq. (5), we take the spectral acoustic particle

velocity $\tilde{v}_p$ and the spectral acoustic vertical traction $\tilde{t}_k = \Delta_{k3pq}\tilde{r}_{pq}$. These state quantities are continuous across a horizontal source-free interface. Upon eliminating the in-plane components of the acoustic stress, we obtain the following coupled system of first-order ordinary differential equations

$$\partial_3\tilde{\mathsf{f}} + s\tilde{\mathsf{A}}\tilde{\mathsf{f}} = \tilde{\mathsf{n}}, \tag{7}$$

where $\tilde{\mathsf{f}}$ and $\tilde{\mathsf{A}}$ denote the acoustic-field 6-vector and the 6 by 6 system's matrix, which have the following structure

$$\tilde{\mathsf{f}} = \begin{pmatrix} \tilde{\mathbf{v}} \\ -\tilde{\mathbf{t}} \end{pmatrix} \qquad \text{and} \qquad \tilde{\mathsf{A}} = \begin{pmatrix} \tilde{A}_{11} & \tilde{A}_{12} \\ \tilde{A}_{21} & \tilde{A}_{22} \end{pmatrix}, \tag{8}$$

in which $\tilde{\mathbf{v}}$ and $\tilde{\mathbf{t}}$ are the vector representations for the acoustic particle velocity and the acoustic traction, while the components of the 3 by 3 submatrices of the system's matrix are given by

$$(\tilde{A}_{11})_{ip} = -(c_{\cdot 3\cdot 3})^{-1}_{ik}c_{k3p\lambda}i\alpha_\lambda, \quad (\tilde{A}_{12})_{ip} = (\tilde{A}_{12})_{pi} = (c_{\cdot 3\cdot 3})^{-1}_{ip}, \tag{9a}$$

$$(\tilde{A}_{21})_{ip} = (\tilde{A}_{21})_{pi} = k_{i\mu p\lambda}\alpha_\mu\alpha_\lambda + \rho_{ip}, \quad (\tilde{A}_{22})_{ip} = -i\alpha_\mu c_{i\mu j3}(c_{\cdot 3\cdot 3})^{-1}_{jp}, \tag{9b}$$

in which

$$(c_{\cdot 3\cdot 3})^{-1}_{ik}c_{k3j3} = \delta_{ij} \qquad \text{and} \qquad k_{impq} = c_{impq} - c_{im\jmath 3}(c_{\cdot 3\cdot 3})^{-1}_{\jmath k}c_{k3pq}, \tag{10}$$

respectively. In Eq. (7), we have further introduced the in-layer notional source vector

$$\tilde{\mathsf{n}} = \begin{pmatrix} \tilde{\mathbf{n}}^v \\ \tilde{\mathbf{n}}^\tau \end{pmatrix} \qquad \text{with} \qquad \begin{aligned} \tilde{n}^v_i &= (c_{\cdot 3\cdot 3})^{-1}_{ij}c_{j3\lambda k}\tilde{h}_{\lambda k}, \\ \tilde{n}^\tau_i &= \tilde{f}_i + i\alpha_\mu k_{i\mu pq}\tilde{h}_{pq}. \end{aligned} \tag{11}$$

To solve Eq. (7) we first write $\tilde{\mathsf{f}} = \tilde{\mathsf{C}}\tilde{\mathsf{w}}$, where $\tilde{\mathsf{w}}$ is called the wavevector and $\tilde{\mathsf{C}}$ is a nonsingular transformation matrix. Note that this relation is usually referred to as the composition relation and accordingly $\tilde{\mathsf{C}}$ is referred to as the composition matrix. Choosing $\tilde{\mathsf{C}}$ to be independent of x_3, we substitute $\tilde{\mathsf{f}} = \tilde{\mathsf{C}}\tilde{\mathsf{w}}$ into Eq. (7) and subsequently carry out the substitution

$$\tilde{\mathsf{A}}\tilde{\mathsf{C}} = \tilde{\mathsf{C}}\tilde{\Gamma}, \tag{12}$$

after which we multiply the result on the left by the decomposition matrix $\tilde{\mathsf{D}} = \tilde{\mathsf{C}}^{-1}$, so as to arrive at

$$\partial_3\tilde{\mathsf{w}} + s\tilde{\Gamma}\tilde{\mathsf{w}} = \tilde{\mathsf{e}}, \tag{13}$$

where we have introduced the so-called in-layer excitation vector $\tilde{\mathsf{e}} = \tilde{\mathsf{D}}\tilde{\mathsf{n}}$. Now, observe that Eq. (13) comprises a decoupled system of six first order differential equations, provided that $\tilde{\Gamma}$ is a diagonal matrix. But if we require that $\tilde{\Gamma}$ is a diagonal matrix, then Eq. (12) must denote an eigenvalue problem and $\tilde{\mathsf{A}}$ must be a simple matrix. Moreover, the columns of $\tilde{\mathsf{C}}$ are eigencolumns of $\tilde{\mathsf{A}}$ and the assumption that $\tilde{\mathsf{C}}$ may be chosen independent of x_3 within the interval $\mathcal{I}_J$ is justified, since the system's matrix $\tilde{\mathsf{A}}$ itself is independent of x_3 in this interval.

Before we can explore the structure of the composition matrix, we have to investigate the structure of the system's matrix as given by Eqs. (8)-(9). First, for $\alpha_\mu \in \mathbb{R}^2$, the system's matrix is Hamiltonian, i.e.,

$$\tilde{A}_{12} \overset{\mathrm{H}}{=} \tilde{A}^H_{12} \qquad \tilde{A}_{21} \overset{\mathrm{H}}{=} \tilde{A}^H_{21} \qquad \tilde{A}_{22} \overset{\mathrm{H}}{=} -\tilde{A}^H_{11} \tag{14}$$

where the superscript H denotes the operation of Hermitean transposition. Secondly, the matrix $\tilde{A}_{12}$ is positive definite, while for $\alpha_\mu \in \mathbb{R}^2$ the matrix $\tilde{A}_{21}$ is positive definite as well. Thirdly, for the reciprocal media under consideration, the system's matrix is K-symmetric, i.e.,

$$\tilde{A}_{12} \overset{\mathrm{K}}{=} \tilde{A}^T_{12} \qquad \tilde{A}_{21} \overset{\mathrm{K}}{=} \tilde{A}^T_{21} \qquad \tilde{A}_{22} \overset{\mathrm{K}}{=} \tilde{A}^T_{11}, \tag{15}$$

where the superscript T denotes the operation of transposition.

In view of the first two properties of the system's matrix, its eigenvalues $\gamma_{(i)}$, which represent the vertical slownesses, may be classified and arranged in 3 by 3 matrices according to

$$\tilde{\Gamma}^{+} = \mathrm{diag}(\gamma_{(1)}, \gamma_{(2)}, \gamma_{(3)}), \quad \text{with} \quad \mathrm{Re}(\gamma_{(3)}) \geq \mathrm{Re}(\gamma_{(2)}) \geq \mathrm{Re}(\gamma_{(1)}) > 0, \tag{16a}$$

$$\tilde{\Gamma}^{-} = \mathrm{diag}(\gamma_{(4)}, \gamma_{(5)}, \gamma_{(6)}), \quad \text{with} \quad \gamma_{(i+3)} = -(\gamma_{(i)})^{*}, \quad \text{for} \quad i = 1, 2, 3, \tag{16b}$$

where the superscript $*$ denotes the operation of complex conjugation. Consequently, we rewrite the eigenvalue matrix, the wavevector and the in-layer excitation vector in terms of 3 by 3 matrices and 3-vectors according to

$$\tilde{\Gamma} = \begin{pmatrix} \tilde{\Gamma}^{+} & \mathsf{O} \\ \mathsf{O} & \tilde{\Gamma}^{-} \end{pmatrix}, \qquad \tilde{\mathbf{w}} = \begin{pmatrix} \tilde{\mathbf{w}}^{+} \\ \tilde{\mathbf{w}}^{-} \end{pmatrix} \qquad \text{and} \qquad \tilde{\mathbf{e}} = \begin{pmatrix} \tilde{\mathbf{e}}^{+} \\ \tilde{\mathbf{e}}^{-} \end{pmatrix}, \tag{17}$$

respectively.

As a result of all three properties of $\tilde{\mathsf{A}}$ mentioned above, the composition matrix may always be cast in the following form

$$\tilde{\mathsf{C}} = \begin{pmatrix} E & -E \\ \tilde{Z}^{+} & -\tilde{Z}^{-} \end{pmatrix} \begin{pmatrix} \tilde{V}^{+} & \mathsf{O} \\ \mathsf{O} & \tilde{V}^{-} \end{pmatrix}, \tag{18}$$

where E denotes the 3 by 3 identity matrix, while $\tilde{Z}^{+}$ and $\tilde{Z}^{-}$ denote the impedance matrices for the down- and up-going wave motion, respectively. Moreover, $\tilde{Z}^{-} = -(\tilde{Z}^{+})^{T}$, while for $\alpha_{\mu} \in \mathbb{R}^{2}$, the matrices $\tilde{Z}^{+}$ and $-\tilde{Z}^{-}$ are Hermitean positive definite. Further, the 3 by 3 particle-velocity matrices $\tilde{V}^{+}$ and $\tilde{V}^{-}$ follow from the one-way eigenrelations

$$\tilde{A}^{\pm}\tilde{V}^{\pm} = \tilde{V}^{\pm}\tilde{\Gamma}^{\pm} \quad \text{with} \quad \tilde{A}^{\pm} = \tilde{A}_{11} + \tilde{A}_{12}\tilde{Z}^{\pm} \tag{19}$$

and they are related through $\tilde{V}^{-}(-\alpha_{\mu}) = \tilde{V}^{+}(\alpha_{\mu})$. Upon choosing the so-called power-flux normalization, we have $(\tilde{V}^{\pm})^{T}(\tilde{Z} + \tilde{Z}^{T})\tilde{V}^{\pm} = E$.

It can be shown that the impedance matrices satisfy matrix algebraic Riccati equations, which can be solved by first solving the eigenrelation given by Eq. (12). There is an analytic alternative to this, which enables us to derive important properties of the pertaining quantities without having to solve the corresponding eigenvalue problem explicitly. To this end, we introduce the splitting matrix according to

$$\tilde{\mathsf{B}}(\alpha_{\mu}) = \frac{1}{\pi}\int_{\mathcal{L}} [-i\alpha_{3}\mathsf{E} + \tilde{\mathsf{A}}(\alpha_{\mu})]^{-1}\,\mathrm{d}\alpha_{3} = \tilde{\Pi}^{+} - \tilde{\Pi}^{-}, \tag{20}$$

in which $\tilde{\Pi}^{+}$ and $\tilde{\Pi}^{-}$ are the orthogonal projectors onto the invariant subspaces associated with the eigenvalues of $\tilde{\mathsf{A}}$ with a positive and negative real part, respectively, while the contour $\mathcal{L}$ represents any contour that can be obtained via a continuous deformation — preserving the direction of integration — of the real α_{3}-axis within the domain where the integrand is analytic, provided that the resulting integral comprises a principal-value integral at infinity. From this integral representation, it follows that the splitting matrix inherits the symmetry properties of the system's matrix. In particular $\tilde{\mathsf{B}}$ is both Hamiltonian and K-symmetric, while the off-diagonal submatrices $\tilde{B}_{12}$ and $\tilde{B}_{21}$ are positive definite for $\alpha_{\mu} \in \mathbb{R}^{2}$. Further, it can be shown that $\tilde{\mathsf{B}}$ commutes with $\tilde{\mathsf{A}}$, that 1 and -1 are the threefold eigenvalues of $\tilde{\mathsf{B}}$ and that $\tilde{\mathsf{B}}$ is simple regardless of whether $\tilde{\mathsf{A}}$ is simple or not. Most importantly, the impedance matrices follow from

$$\tilde{Z}^{\pm} = (\tilde{B}_{12})^{-1}(\pm E - \tilde{B}_{11}). \tag{21}$$

The splitting matrix is closely related to the Barnett-Lothe tensor which has proven to be extremely useful in the analysis of surface waves (cf. Chadwick and Smith [10]).

With reference to Eqs. (13) and (17) the solution to the uncoupled system of six first-order differential equations for $x_3 \in \mathcal{I}_J = (x_{3;J-1}, x_{3;J})$ is found to be

$$\tilde{\mathbf{w}}^+(x_3) = \exp[-s(x_3 - x_{3;J-1})\tilde{\Gamma}^+]\tilde{\mathbf{w}}_J^+ + \int_{x_3'=x_{3;J-1}}^{x_3} \exp[-s(x_3 - x_3')\tilde{\Gamma}^+]\tilde{\mathbf{e}}^+(x_3')\,\mathrm{d}x_3', \quad (22a)$$

$$\tilde{\mathbf{w}}^-(x_3) = \exp[-s(x_3 - x_{3;J})\tilde{\Gamma}^-]\tilde{\mathbf{w}}_J^- - \int_{x_3'=x_3}^{x_{3;J}} \exp[-s(x_3 - x_3')\tilde{\Gamma}^-]\tilde{\mathbf{e}}^-(x_3')\,\mathrm{d}x_3', \quad (22b)$$

in which

$$\tilde{\mathbf{w}}_J^+ = \lim_{x_3 \downarrow x_{3;J-1}} \tilde{\mathbf{w}}^+(x_3) \quad \text{and} \quad \tilde{\mathbf{w}}_J^- = \lim_{x_3 \uparrow x_{3;J}} \tilde{\mathbf{w}}^-(x_3) \quad (23)$$

denote the vectorial wave amplitudes of the pertaining wavevectors, respectively. From Eqs. (16) and (22), we infer that the wavevector, thus constructed, remains finite in the limit of s approaching infinity, thus ensuring the causality of the corresponding space-time-domain quantities. Hence, $\tilde{\mathbf{w}}^+$ and $\tilde{\mathbf{w}}^-$ represent the wavevector constituents associated with the down- and up-going wave motion, while $\tilde{\mathbf{e}}^+$ and $\tilde{\mathbf{e}}^-$ represent the in-layer excitation-vector constituents that excite down- and up-going wave constituents, respectively.

To obtain a causal description of the interaction of the space-time-domain wavefield quantities at either side of a horizontal interface, the scattering formalism is ideally suited. To describe the scattering formalism, let us define the modified vectorial wave amplitudes by

$$\check{\mathbf{w}}_J^+ = \lim_{x_3 \uparrow x_{3;J}} \tilde{\mathbf{w}}^+(x_3) \quad \text{and} \quad \check{\mathbf{w}}_J^- = \lim_{x_3 \downarrow x_{3;J-1}} \mathbf{w}^-(x_3). \quad (24)$$

In terms of the quantities defined above, the scattering of the waves at the interface located at the vertical level $x_3 = x_{3;J}$ is described by

$$\begin{pmatrix} \tilde{\mathbf{w}}_{J+1}^+ \\ \tilde{\mathbf{w}}_J^- \end{pmatrix} = \tilde{\mathsf{S}}_J \begin{pmatrix} \check{\mathbf{w}}_{J+1}^- \\ \check{\mathbf{w}}_J^+ \end{pmatrix} \qquad \text{with} \qquad \tilde{\mathsf{S}}_J = \begin{pmatrix} \tilde{S}_J^{+;-} & \tilde{S}_J^{+;+} \\ \tilde{S}_J^{-;-} & \tilde{S}_J^{-;+} \end{pmatrix}, \quad (25)$$

in which the scattering matrix $\tilde{\mathsf{S}}_J$ pertaining to the level $x_3 = x_{3;J}$ may be expressed in terms of the impedance matrices and the particle-velocity matrices according to

$$\tilde{\mathsf{S}}_J = \begin{pmatrix} (\tilde{V}_{J+1}^+)^{-1} & \mathsf{O} \\ \mathsf{O} & (\tilde{V}_J^-)^{-1} \end{pmatrix} \begin{pmatrix} (\tilde{Z}_{J+1} + \tilde{Z}_J^T)^{-1}(\tilde{Z}_J^T - \tilde{Z}_{J+1}^T) & (\tilde{Z}_{J+1} + \tilde{Z}_J^T)^{-1}(\tilde{Z}_J + \tilde{Z}_J^T) \\ (\tilde{Z}_{J+1} + \tilde{Z}_J^T)^{-1}(\tilde{Z}_{J+1} + \tilde{Z}_{J+1}^T) & (\tilde{Z}_{J+1} + \tilde{Z}_J^T)^{-1}(\tilde{Z}_{J+1} - \tilde{Z}_J) \end{pmatrix} \times \begin{pmatrix} \tilde{V}_{J+1}^- & \mathsf{O} \\ \mathsf{O} & \tilde{V}_J^+ \end{pmatrix}. \quad (26)$$

At a free surface bounding the configuration from above, we simply have

$$\mathbf{w}_1^+ = -(\tilde{V}_1^+)^{-1}\tilde{Z}_1^{-1}\tilde{Z}_1^T\tilde{V}_1^-\check{\mathbf{w}}_1^- + (\tilde{V}_1^+)^{-1}\tilde{Z}_1^{-1}\mathbf{n}_0^\tau, \quad (27)$$

where the notional source term $\mathbf{n}_0^\tau$ accounts for the action of a force source at the free surface.

4. THE RADIATION FROM A BOREHOLE

To determine the radiation emanating from a fluid-filled cased borehole, we employ a small parameter analysis. Such an analysis has previously been employed by Burridge *et al.* [7] to investigate the wavefield radiated into an arbitrary anisotropic homogeneous formation from an uncased hole. For brevity, we restrict ourselves to discussing the analysis pertaining to transversely isotropic media with a preferred direction along the vertical (TIV media).

The linearized equation of motion and the deformation rate equation governing the acoustic wave motion in the borehole fluid in the presence of a point source of volume injection at $x_m = x_m^S$ are given by

$$\partial_k p + \rho^{\mathrm{f}} \partial_t w_k = 0, \tag{28a}$$

$$\partial_k w_k + \kappa^{\mathrm{f}} \partial_t p = Q(t)\delta(x_m - x_m^S), \tag{28b}$$

in which p is the acoustic pressure (Pa), w_m is the particle velocity (m/s) in the fluid, ρ^{f} is the fluid volume density of mass (kg/m^3), κ^{f} is the fluid compressibility (Pa^{-1}) and $Q = Q(t)$ is the time-rate of volume injection (m^{3}s^{-1}) of the point source. Further it is convenient to employ the generalized Hooke's law instead of the deformation rate equation in the solid, i.e.,

$$\Delta_{ijpq}\partial_q u_p - \varsigma_{ijpq}\tau_{pq} = 0, \tag{29}$$

where the particle displacement u_p (m) is related to the particle velocity in the solid via $v_m = \partial_t u_m$. We assume that the outer radius b^+ of the outermost shell is small compared to the wavelength, or, equivalently that the traveltime across a borehole may be neglected compared to the width of the typical time window in which the wave phenomena of interest take place. To express this, we introduce the new variables

$$x'_\mu = x_\mu, \quad x'_3 = \epsilon x_3, \quad t' = \epsilon t, \tag{30}$$

where ϵ is a small parameter (cf. Burridge *et al.* [7]). Accordingly, we represent all field quantities in terms a power series expansion in the small parameter, according to

$$\tau_{pq} = \sum_{n=0}^{\infty} \tau_{pq}^{(n)}, \quad u_m = \sum_{n=0}^{\infty} u_m^{(n)}, \quad p = \sum_{n=0}^{\infty} p^{(n)} \quad \text{and} \quad w_m = \sum_{n=0}^{\infty} w_m^{(n)}, \tag{31}$$

where

$$\tau_{pq}^{(n)} = \epsilon^n \tau_{pq}'^{(n)}, \quad u_m^{(n)} = \epsilon^n u_m'^{(n)}, \quad p^{(n)} = \epsilon^n p'^{(n)} \quad \text{and} \quad w_m^{(n)} = \epsilon^n w_m'^{(n)}, \tag{32}$$

respectively. After substitution of Eqs. (30)-(31) into Eqs. (1a), (28) and (29), we obtain a series of differential equations. Upon collecting the terms with equal powers of ϵ, we arrive at an infinite set of differential equations for the coefficients in Eq. (31). Knowing the order of these coefficients, we may recast the equations in terms of the original coordinates and subsequently solve the equations for ascending orders of ϵ. Before we present the results of this analysis, let us define the radial stiffness according to

$$\eta(b) = \frac{-\tau_{\lambda\mu}\nu_\lambda\nu_\mu}{bu_\kappa\nu_\kappa}, \tag{33}$$

where b denotes the radial distance to the centre of the borehole. Note that the radial stiffness is continuous across all interfaces.

The equations for $O(\epsilon^0)$ pertaining to the fluid wave motion show that $p^{(0)}$ and $w_3^{(0)}$ are constant over a cross-section of the borehole fluid, and that $w_\lambda^{(0)}$ vanishes identically. Investigation of the fluid/solid boundary conditions for $O(\epsilon^0)$ yields $p^{(0)}\delta_{m\mu}\nu_\mu = -\Delta_{m\lambda kr}\nu_\lambda\tau_{kr}^{(0)}$ at the fluid/solid interface. To satisfy the boundary conditions for $O(\epsilon^0)$ at the interfaces between the circular cylindrical shells it is required that $u_m^{(0)}$ and $\Delta_{i\lambda kr}\nu_\lambda\tau_{kr}^{(0)}$ are continuous across these interfaces. Further, $u_m^{(0)}$ should vanish for $(x_\mu x_\mu)^{1/2} \to \infty$. Together with the boundary conditions, the equations for $O(\epsilon^0)$ pertaining to the solid comprise a planar quasi-static problem in $\tau_{\lambda\mu}^{(0)}$, $\tau_{33}^{(0)}$ and $u_\lambda^{(0)}$, with $p^{(0)}$ as the scalar amplitude forcing function. After having solved the quasi-static problem within each of the cylindrical shells, we can derive a backward recurrence scheme to obtain the radial stiffness at consecutive interfaces starting at $\eta_N = 2c_{1212}$ for $b = b^+$ at the outer wall (cf. De Hoop *et al.* [8]).

To satisfy the boundary conditions for $O(\epsilon^1)$ at the interfaces between the circular cylindrical shells it is required that $u_m^{(1)}$ and $\Delta_{i\lambda kr}\nu_\lambda \tau_{kr}^{(1)}$ are continuous across these interfaces. Further, we may treat the solid equation of motion for $O(\epsilon^1)$ in the integral sense according to

$$-\int_{x_\mu\in\partial\mathcal{S}} \Delta_{j\lambda kr}\nu_\lambda \tau_{kr}^{(1)}\,\mathrm{d}\ell = \int_{\substack{x_\mu\in\mathcal{B}^+\setminus\mathcal{B}^- \\ x_3\text{fixed}}} \Delta_{j3kr}\partial_3 \tau_{kr}^{(0)}\,\mathrm{d}\Sigma. \tag{34}$$

Investigation of the fluid/solid boundary conditions for $O(\epsilon^1)$ yields $p^{(1)}\delta_{m\mu}\nu_\mu = -\Delta_{m\lambda kr}\nu_\lambda\tau_{kr}^{(1)}$ and $\nu_\lambda\partial_t u_\lambda^{(0)} = \nu_\lambda w_\lambda^{(1)}$ at the fluid/solid interface. The equations for $O(\epsilon^1)$ pertaining to the fluid wave motion lead to the following waveguide-mode equations for the so-called tube wave

$$\partial_3 p^{(0)} + \rho\partial_t w_3^{(0)} = 0 \tag{35}$$

$$\partial_3 w_3^{(0)} + (\kappa + 2/\eta_1)\partial_t p^{(0)} = Q(t)\delta(x_3 - x_3^S) \tag{36}$$

where η_1 is the radial stiffness at the fluid/solid interface.

The solution to the Laplace-transform-domain counterpart of Eq. (36) is found to be

$$\{\hat{p}^{(0)}; \hat{w}_3^{(0)}\} = \begin{cases} P\exp[-s\gamma_T(x_3 - x_3^S)]\,\{1; \gamma_T/\rho^{\mathrm{f}}\} & \text{for} \quad x_3 > x_3^S, \\ P\exp[s\gamma_T(x_3 - x_3^S)]\,\{1; -\gamma_T/\rho^{\mathrm{f}}\} & \text{for} \quad x_3 < x_3^S, \end{cases} \tag{37}$$

where $\gamma_T = (\rho^{\mathrm{f}}\kappa^{\mathrm{f}} + 2\rho^{\mathrm{f}}/\eta_1)^{1/2}$ and $P = \rho^{\mathrm{f}}\hat{Q}(s)/(2\Omega^-\gamma_T)$ denote the tube-wave slowness and the modal pressure amplitude, respectively. Having determined the fluid wavefield quantities, we may apply a quasi-static recurrence scheme (cf. De Hoop *et al.* [8]) to obtain the $O(\epsilon^1)$ coefficients of the traction and particle displacement on the outer interface $\partial\mathcal{B}^+$.

Next, let us examine the spectral surface sources defined in Eq. (6). To this end, we express the Fourier kernel as $\exp(is\alpha_\lambda x_\lambda^0)\exp(is\alpha_\lambda\nu_\lambda b^+)$, in which x_λ^0 denotes the horizontal coordinates at the centre of the borehole. Since, $|s\alpha_\mu|$ is inversely proportional to the wavelength, we have $is\alpha_\mu\nu_\mu b^+ = O(\epsilon)$. Hence, we may rewrite the Fourier kernel according to

$$\exp(is\alpha_\lambda x_\lambda^0)[1 + is\alpha_\lambda\nu_\lambda b^+ + O(\epsilon^2)]. \tag{38}$$

Upon substituting both Eq. (38) and the expressions for the normal stress and the radial component of the particle velocity, which follow from the quasi-static recurrence scheme, into Eq. (6), we can analytically evaluate the integrals along the pertaining cross-sectional circular boundary, yielding the leading-order in-plane components of the spectral-domain boundary-surface sources. The calculation of $\tilde{h}_{3\lambda}^{\partial\mathcal{B}^+} = \tilde{h}_{\lambda 3}^{\partial\mathcal{B}^+}$ would require that we evaluate the vertical component of the particle velocity at $\partial\mathcal{B}^+$. Fortunately, it turns out that the pertaining source contribution is more than one order of ϵ smaller than the in-plane source terms, and may hence be discarded. However, in the presence of an axisymmetric TIV shell structure surrounding the fluid-filled hole, the vertical component of the boundary-surface-force source containing $\tau_{3\lambda}^{(1)}$ and the in-plane boundary-surface sources containing $\tau_{\mu\lambda}^{(0)}$ are of the same order in ϵ. However, as $\tau_{kr}^{(0)}$ is known throughout the shell structure, we may employ Eq. (34) to calculate $\tilde{f}_3^{\partial\mathcal{B}^+}$ in closed form as well. As a result, we are left with line integrals (cf. Eq. (22)) along vertical segments, which describe the tube-wave radiation into the formation.

Across the vertical levels $x_3 = x_{3;J}$ at which the interfaces between two solids are located, the radial stiffness and hence the tube-wave slowness jump. As a consequence, an incident tube wave will be scattered at the pertaining level. Imposing the condition that the leading order acoustic pressure $\hat{p}^{(0)}$ and axial volume flow $\Omega^-\hat{w}_3^{(0)}$ be continuous across the pertaining level (cf. White [11]), leads to a standard one-dimensional scattering formalism for the tube waves. Note that at such a level the corresponding boundary-surface sources cease to be analytical, which gives

rise to strong *secondary* borehole source contributions.

5. THE RECEIVED ACOUSTIC PRESSURE

To construct the full spectral wavefield at a certain vertical level, we first observe that the superposition principle holds. Hence, we may regard the overall wavefield as consisting of the sum of individual wavefield constituents that — after their excitation — have undergone successive reflections and transmissions in the process of propagating through the medium. An individual wavefield constituent that has interacted ϖ times at the interfaces is referred to as a generalized-ray constituent of the order ϖ, also known as a generalized ray (cf. Spencer [12]).

The next step, is to construct the full spectral acoustic pressure at the receiver level on the axis of the receiving borehole. To do this, we employ the reciprocity theorem for acoustic wavefields in fluid/solid configurations. The key to the pertaining analysis is the introduction of an auxiliary state, for which we take the wavefield as it would be generated by a point source of volume injection located at the point where we want to evaluate the received acoustic pressure. For a detailed description, we refer to De Hoop *et al.* [8]. The analysis leads to

$$\hat{p}(\mathbf{x}^R) = \Delta_{ijpq} \int_{\mathbf{x}^R \in \partial\mathcal{B}_R^+} [-\hat{\tau}_{pq}^{\mathrm{in}} \hat{v}_i^R + \hat{\tau}_{pq}^R \hat{v}_i^{\mathrm{in}}] \nu_j \, \mathrm{d}\Sigma. \tag{39}$$

Subsequently, we use Eq. (4) to express the Laplace-transform-domain incident wavefield quantities at the wall of the receiving borehole in terms of their spectral counterparts, after which we interchange the order of integration. In analogy with the transmitting situation for TIV media, the resulting integrals in the cross-sectional plane can be evaluated analytically yielding explicit expressions for the boundary-surface receivers $\tilde{f}_k^{\partial\mathcal{B}_R^+}$ and $\tilde{h}_{ij}^{\partial\mathcal{B}_R^+}$, respectively. Further, upon introducing $\Lambda_{ij} = \delta_{i\mu}\delta_{\mu j} - \delta_{i3}\delta_{3j}$ and employing certain symmetry relations, we finally obtain

$$\tilde{p}(\alpha_\mu, x_3^R) = \exp(is\alpha_\mu x_\mu^R) \int -\tilde{\tau}_{ij}^{\mathrm{in}} \Lambda_{im} \Lambda_{jn} \tilde{h}_{mn}^{\partial\mathcal{B}_R^+} + \tilde{f}_i^{\partial\mathcal{B}_R^+} \Lambda_{ij} \tilde{v}_j^{\mathrm{in}} \, \mathrm{d}x_3, \tag{40}$$

where the integral is carried out along the axis of the receiving borehole.

6. THE SPACE-TIME-DOMAIN QUANTITIES

The parameters of integration in the line integrals describing the tube-wave radiation into the formation and the reciprocal reception of the elastic wavefield by the tube waves in the receiving hole only occur as linear factors in the arguments of the exponentials associated with the vertical propagation. Hence, these integrals can be evaluated analytically, leaving us with the contributions from the end points of the intervals of integration. To each single contribution to the received acoustic pressure, there corresponds a time delay t_{del} associated with the tube-wave propagation. Consequently, an individual spectral generalized-ray Green's-function constituent $\tilde{G}$ and the time domain acoustic pressure may be cast in the following generic form

$$\tilde{G} = s^2\tilde{g} = 4\pi^2 \exp(-st_{\mathrm{del}}) \exp(-s\textstyle\sum h\gamma)\tilde{\chi}(\alpha_\mu) \quad \rightarrow \quad p^R(\mathbf{x}^R, t) = \sum_{\substack{\text{generalized} \\ \text{rays}}} g \overset{t}{*} \partial_t^2 Q(t), \tag{41}$$

where $\exp(-s\sum h\gamma)$ is representative of the down- and upward propagation through the consecutive layers, $\tilde{\chi}$ describes the excitation by a primary or secondary tube-wave source, the scattering at the interfaces and the reception by a primary or secondary tube-wave receiver, while $\overset{t}{*}$ denotes the convolution with respect to time. Now, let us formally apply the inverse Fourier transformation on $\tilde{g}$ (cf. Eq. (4)). Upon employing the polar coordinates $\alpha_1 = -ip\cos(\psi)$, $\alpha_2 = -ip\sin(\psi)$,

with $d\alpha_1 d\alpha_2 = -pdpd\psi$, we obtain the Laplace-transform-domain counterpart of $\tilde{g}$

$$\hat{g} = -\mathrm{Re} \int_{\psi=0}^{\pi} \int_{p=0}^{i\infty} \exp(-st)\check{\chi}(p,\psi)\, p\, \mathrm{d}p\, \mathrm{d}\psi, \tag{42}$$

where p represents the horizontal slowness, $t = t(p,\psi) = pr\cos(\psi) + \sum h\gamma(p,\psi)$ is a complex parameter with the dimension of time, r denotes the horizontal offset between the source and receiving holes and $\check{\chi}(p,\psi) = \tilde{\chi}[\alpha_\mu(p,\psi)]$, respectively. To return to the space-time domain, we employ the Cagniard-de Hoop method in polar coordinates. For a detailed description of this method, we refer to Van der Hijden [9]. Here, we mention the crucial steps in the method. First, for ψ fixed, we deform the contour of integration such that t is real and increases along the contour. This contour of integration is unique and is known as the Cagniard contour. Next, we map t to p and replace the parameter of integration p by t. Subsequently, we interchange the order of integration, after which the space-time-domain counterpart of $\hat{g}$ may be recognized by inspection. This procedure leads to

$$g = \mathrm{Re} \int_{\psi=0}^{\pi} -\check{\chi}[p(t,\psi),\psi]\, p(t,\psi)\partial_t p(t,\psi)\, \mathrm{d}\psi. \tag{43}$$

To show that the deformation of the contour of integration into the complex p-plane is allowed, the analytical properties of the splitting matrix $\tilde{B}[\alpha_\mu(p,\psi)]$ in the complex p-plane can be employed. It turns out that the only singularities of $\tilde{B}$ in the complex p-plane are branch points located on the real p-axis. Further, upon identifying a slowness with a reciprocal speed, it can be shown that the matrix $-i\tilde{B}$, evaluated at an infinitesimal distance above the real p-axis and beyond the outermost branch point, is related to a particular realization of the so-called Barnett-Lothe tensor via a similarity transformation. Finally, the integral representation for the splitting matrix may be used to show that Rayleigh-wave poles must be located on the real p-axis.

6.1. An alternative implementation of the modified Cagniard method for TIV-symmetric stratified media

Below, we present a numerically expedient alternative to the ψ-integral. For TIV media both the vertical slownesses and $\check{\chi}$ are independent of ψ. So, performing the ψ-integral for t fixed, p and ψ have to satisfy

$$t = pr\cos(\psi) + \sum h\gamma(p). \tag{44}$$

Hence, as ψ runs from 0 to π, the horizontal slowness traces out a path in the complex p-plane, starting at $p = p_b$ and ending at $p = p_e = -p_b^*$, where p_b and p_e are the horizontal slownesses that satisfy

$$t = p_b r + \sum h\gamma(p_b) \qquad \text{and} \qquad t = -p_e r + \sum h\gamma(p_e), \tag{45}$$

respectively. Now, we change the variable of integration from ψ to p. As t is fixed, taking the differential of Eq. (44) leads to

$$0 \equiv \mathrm{d}t = \partial_p t\, \mathrm{d}p - pr\sin(\psi)\, \mathrm{d}\psi, \quad \rightarrow \quad \mathrm{d}\psi = [pr\sin(\psi)]^{-1}|_{\psi=\psi(p)} \partial_p t\, \mathrm{d}p. \tag{46}$$

A Cagniard contour never enters the lower half of the complex p-plane. Hence, we may write

$$pr\sin(\psi) = i[p^2r^2\cos^2(\psi) - p^2r^2]^{\frac{1}{2}} = i[(t - \sum h\gamma)^2 - p^2r^2]^{\frac{1}{2}}, \tag{47}$$

in which the real part of the square root is taken nonnegative and we have used Eq. (44).

Now, let C_ψ^t denote the segment of the Cagniard contour C_ψ that starts at $p = 0$ and ends at $p = p(t,\psi)$, being the horizontal slowness that corresponds to the time t. Then, we may deform

Experiment no.	Elastic properties (in GPa and kg/m^3)					
	c_{11}	c_{33}	c_{13}	c_{44}	c_{66}	ρ^{f}
1	295	335	111	71	68	8900
2	95.9364	95.9364	19.8716	38.0324	38.0324	3290

Table 1: The elastic properties of the formation pertaining to the two experiments

the contour of integration in the complex p-plane — keeping the end points p_b and p_e fixed — in such a way that p traces out $\mathcal{C}_0^t$ in the opposite direction until it reaches the origin, after which p traces out $\mathcal{C}_\pi^t = (-\mathcal{C}_0^t)^*$. As a consequence of the contour deformation described above, Eq. (43) becomes

$$g(x_m, x_3', t) = \mathrm{Im}\left\{\int_{p\in\mathcal{C}_0^t} - \int_{p\in\mathcal{C}_\pi^t}\right\} p\,\check{\chi}(p,t)\,[(t-\textstyle\sum h\gamma)^2 - p^2r^2]^{-\frac{1}{2}}\,\mathrm{d}p, \tag{48}$$

where $\check{\chi}(p,t) = \check{\chi}[p,\psi(t,p)]$ and we have used the elementary property $\mathrm{Re}[-i(\cdots)] = \mathrm{Im}(\cdots)$. The integrand in Eq. (48) is an odd function of p, analytic in the complex p-plane except at the branch points branch cuts and poles and strictly real on the segment of the real p-axis in between the innermost real branchpoint and its opposite. Hence, we may rewrite Eq. (48) according to

$$g(x_m, x_3', t) = 2\mathrm{Im}\int_{p\in\mathcal{C}_0^t} p\,\check{\chi}(p,t)\,[(t-\textstyle\sum h\gamma)^2 - p^2r^2]^{-\frac{1}{2}}\,\mathrm{d}p, \tag{49}$$

which is akin to a representation obtained by Helmberger[13]. The rationale of the above is that we avoid having to evaluate the Cagniard contours for different values of ψ. Moreover, the integrand need only be evaluated at a limited number of points on $\mathcal{C}_0^t$, after which rational interpolation suffices to obtain the values of the integrand at intermediate points.

7. NUMERICAL EXAMPLES

Below we present numerical results pertaining to two different cross-well experiments, one in an anisotropic homogeneous formation and one in an isotropic formation bounded from above by a free surface. The distance between the boreholes in both experiments is 100 m.

For the source signature $\partial_t^2 Q$ with which the Green's functions are convolved, we take the second derivative with respect to time of the following causal pulse (cf. De Hoop *et al.* [14])

$$Q(t) = \begin{cases} 0 & \text{for } t<0, \\ \left(\dfrac{\alpha t}{\nu}\right)^{\nu} \exp(-\alpha t+\nu)\sin(\omega_0 t) & \text{for } t>0, \end{cases} \tag{50}$$

with $\nu = 2$, a pulse width of 5 ms, a centre frequency of 1000rad/s (159.15Hz), a rise time of $\nu/\alpha = 2.7$ms, and unit amplitude at the rise time, respectively.

In both experiments, the boreholes are filled with water with a wavespeed $c = (\rho^{\mathrm{f}}\kappa^{\mathrm{f}})^{-1/2} = 1500$ m/s and a density $\rho_f^{\mathrm{f}} = 1000$ m/s, respectively. Further, the receiving borehole has a perfectly bonded steel casing, with compressional- and shear-wave speeds $c_P = 5750$ m/s and $c_S = 3120$ m/s, and a density $\rho = 7910$ kg/m^3, respectively. The transmitting borehole is uncased. The values of the formation parameters pertaining to the two experiments are listed in Table 1.

In the first experiment, the formation is a homogeneous TIV medium. The constitutive coefficients are those of Cobalt, i.e., the associated real slowness surface belongs to the main class C_{12} in the classification scheme proposed by Chadwick [15]. The qSV sheet of this slowness surface is concave for $0.639 < |\gamma/p| < 1.335$. After projecting the corresponding wave surface from the point where the source is located onto the the axis of the receiving borehole, the cuspidal edges of the wave surface are mapped onto the vertical offsets $x_3^R - x_3^S = 87.87$ m, and $x_3^R - x_3^S = 106.28$ m. We have chosen $x_3^R - x_3^S = 100$ m, so as to obtain an optimum separation of the triplicated events. The cross-hole Green's function and the associated pressure pulse are depicted in Figure 2.

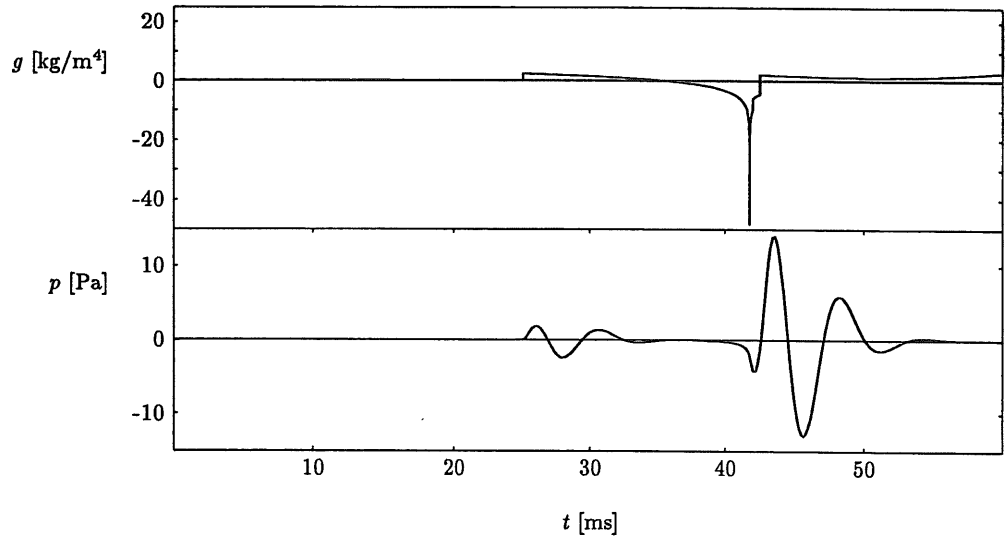

Figure 2: The cross-hole acoustic-pressure Green's function and the the received acoustic pressure pertaining to the first experiment

In the second experiment the isotropic formation is bounded from above by a free surface at the vertical level $x_3 = 0$ m. The source and receiver are located at $x_3^S = 50$ m and $x_3^R = 80$ m, respectively. The constitutive parameters are those of Peridotite 2 found at Kailua, Hawaii. The time window of observation has been chosen such that the Rayleigh wave that is excited by the secondary tube-wave source at the free surface and received by the secondary tube-wave receiver at the free surface, arrives after the final time of observation, as the other events would otherwise be overshadowed due to the large amplitude of this Rayleigh wave. The first two data sets depicted in Figure 3 represent the Green's function and the associated pressure pulse of the primary compressional- and shear-wave. The last two data sets depicted in Figure 3 represent the full Green's function and the associated pressure pulse, i.e., all combinations of primary and secondary sources and receivers and both the direct and the reflected (and converted) wave contributions have been taken into account. For instance, the sharp peeks in the Green's function in the third graph in Figure 3 are due to the coupling between the wavefield radiated by the secondary tube waves at the free surface in the source hole to the primary tube waves at the receiver and to the coupling of the wavefield radiated by the primary tube-wave at the source to the secondary tube waves at the free surface in the receiving hole.

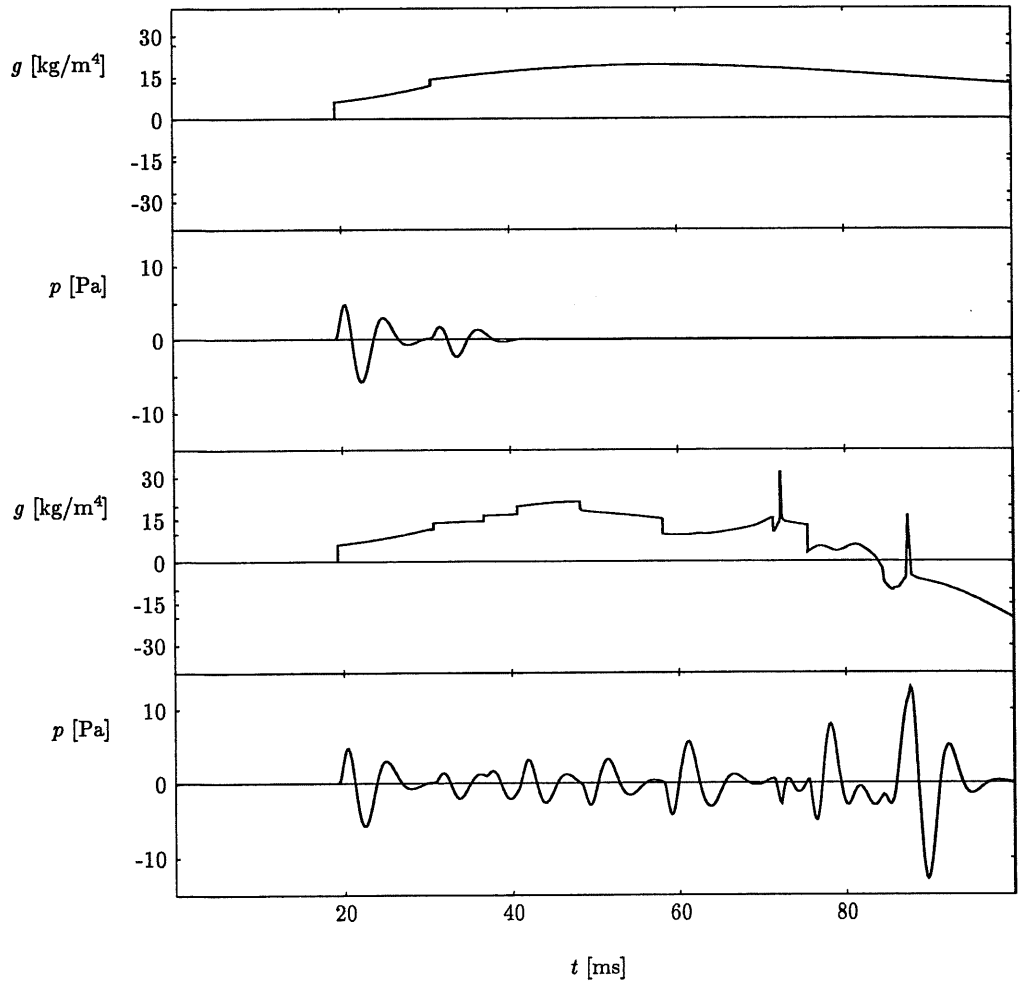

Figure 3: The cross-hole acoustic-pressure Green's function and the received acoustic pressure pertaining to the second experiment; in the two graphs at the top only the primary compressional- and shear-wave contributions are shown.

In stratified formations the cross-hole transient signal transfer contains strong secondary wave contributions. This explains the complexity of the wave phenomena observed in real cross-hole data sets. The method presented in this paper is an efficient method to fully calculate the pertaining cross-hole transient signal transfer for formations consisting of a modest number of horizontal anisotropic layers. From a theoretical point of view, the splitting and impedance matrices as defined in the complex horizontal slowness plane, combined with the alternative implementation of the Cagniard-De Hoop method provides a powerful new modelling tool. The small-parameter analysis is ideally suited for a rigorous investigation of the low-frequency tube-wave motion in a cased borehole embedded in an anisotropic formation.

ACKNOWLEDGMENTS

The research reported in this paper has financially been supported through Research Grants from the Royal/Dutch Shell Exploration and Production Laboratories, Rijswijk The Netherlands; and from the Stichting Fund for Science, Technology and Research (a companion organization to the Schlumberger Foundation in the U.S.A.)

REFERENCES

[1] White, J. E., and Sengbush, R. L., Shear waves from explosive sources, Geophysics, vol. 28, 1963, pp. 1001–1019.

[2] Dong, W., and Toksöz, M. N., Borehole seismic-source radiation in layered isotropic and anisotropic media: Real data analysis, Geophysics, vol. 60, 1995, pp. 748–757.

[3] Lee, M. W., and Balch, A. H., Theoretical seismic wave radiation from a fluid-filled borehole, Geophysics, vol. 47, 1982, pp. 1308-1314.

[4] Meredith, J. A., Numerical and Analytical Modeling of Downhole Seismic Sources: The near and Far Field, Ph.D. thesis, Massachusetts Institute of Technology, Cambridge MA, U.S.A., 1990.

[5] Kurkjian, A. L., De Hon, B. P., White J. E., De Hoop, A. T., and Marzetta T. L., A moving point mechanism representation for low frequency monopole borehole sensors, EAEG Expanded Abstracts, paper P074, Paris, 1992.

[6] Track, A., and Daube, F., Borehole coupling in cross-well wave propagation, EAEG Expanded Abstracts, paper B026, Paris, 1992.

[7] Burridge, R., Kostek, S., and Kurkjian, A. L., Tube waves, seismic waves and effective sources, Wave Motion, vol. 18(2), 1993, pp. 163–210.

[8] De Hoop, A. T., De Hon, B. P., and Kurkjian, A. L., Calculation of transient tube-wave signals in cross-borehole acoustics, J. Acoust. Soc. Am., vol. 95(4), 1994, pp. 1773–1789.

[9] Van der Hijden, J. H. M. T., Propagation of transient elastic waves in stratified anisotropic media, North-Holland series in applied mathematics and mechanics, Elsevier Science Publishers B.V., Amsterdam, The Netherlands, second edition, 1987.

[10] Chadwick P., and Smith, G. D., Foundations of the theory of surface waves in anisotropic elastic materials, In C-S. Yih, editor, Advances in Applied Mechanics, vol. 17, pp. 303–376, Academic Press, New York, U.S.A., 1977.

[11] White, J. E., Seismic waves: radiation transmission and attenuation, McGraw-Hill Book Company, New York, U.S.A., 1965.

[12] Spencer, T. W., The method of generalized reflection and transmission coefficients, Geophysics, vol. 25, 1960, pp. 625–641.

[13] Helmberger, D. V., The crust-mantle transition in the Bering sea, Bulletin of the Seismological Society of America, vol. 58, 1968, pp. 179–214.

[14] De Hoop, A. T. Zeroug, S, and Kostek, S, Transient analysis of the transmitting and receiving properties of a focused acoustic transducer with arbitrary rim, internal report, no. Et/EM 1995-12, Delft University of Technology, Department of Electrical Engineering, Laboratory of Electromagnetic Research, 1995.

[15] Chadwick, P., Wave propagation in transversely isotropic media — I. homogeneous plane waves, Proc. R. Soc. Lond. A, vol. 422, 1989, pp. 23–66.